The EMBO Journal (2011) 30, 706–718 | © 2011 European Molecular Biology Organization | All Rights Reserved 0261-4189/11
www.embojournal.org

THE EMBO JOURNAL

A single immunoglobulin-domain protein required for clustering acetylcholine receptors in *C. elegans*

Georgia Rapti[1,2,3], Janet Richmond[4] and Jean-Louis Bessereau[1,2,3,*]

[1]Biology Department, Ecole Normale Supérieure, IBENS, Paris, France, [2]INSERM U1024, Paris, France, [3]CNRS, UMR 8197, Paris, France and [4]Department of Biological Sciences, University of Illinois at Chicago, Chicago, IL, USA

At *Caenorhabditis elegans* neuromuscular junctions (NMJs), synaptic clustering of the levamisole-sensitive acetylcholine receptors (L-AChRs) relies on an extracellular scaffold assembled in the synaptic cleft. It involves the secreted protein LEV-9 and the ectodomain of the transmembrane protein LEV-10, which are both expressed by muscle cells. L-AChRs, LEV-9 and LEV-10 are part of a physical complex, which localizes at NMJs, yet none of its components localizes independently at synapses. In a screen for mutants partially resistant to the cholinergic agonist levamisole, we identified *oig-4*, which encodes a small protein containing a single immunoglobulin domain. The OIG-4 protein is secreted by muscle cells and physically interacts with the L-AChR/LEV-9/LEV-10 complex. Removal of OIG-4 destabilizes the complex and causes a loss of L-AChR clusters at the synapse. Interestingly, OIG-4 partially localizes at NMJs independently of LEV-9 and LEV-10, thus providing a potential link between the L-AChR-associated scaffold and local synaptic cues. These results add a novel paradigm for the immunoglobulin super-family as OIG-4 is a secreted protein required for clustering ionotropic receptors independently of synapse formation.

The EMBO Journal (2011) **30,** 706–718. doi:10.1038/emboj.2010.355; Published online 21 January 2011
Subject Categories: neuroscience
Keywords: extracellular scaffold; LEV-9; LEV-10; neuromuscular junction

Introduction

At chemical synapses, diffusion and active clearance of neurotransmitter result in a rapid drop in concentration with distance from neurotransmitter release sites. Clustering receptors at synapses is, therefore, critical to efficiently sense the active concentration of neurotransmitter present in the synaptic cleft. Receptor clustering also supports coupling with the specialized transduction machinery that resides in the post-synaptic compartment. Diverse molecular systems have evolved for clustering receptors at the synapse, but in most cases, there is a common theme involving interactions between the receptors and a protein scaffold localized below the plasma membrane. Such a prototypic system is found at the vertebrate NMJ for clustering nicotinic acetylcholine receptors (AChRs) (Sanes and Lichtman, 2001; Song and Balice-Gordon, 2008). The cytoplasmic region of muscle AChRs associates with the myristoylated protein rapsyn, which is present in the post-synaptic membrane of vertebrate NMJs throughout synaptogenesis (reviewed in Huh and Fuhrer, 2002). In *rapsyn*$^{-/-}$ mice, NMJs do not differentiate and AChRs fail to cluster (Gautam *et al*, 1996). At central synapses, synaptic accumulation of neurotransmitter receptors involves similar scaffolding proteins such as gephyrin for glycine and GABA receptors (Kneussel and Loebrich, 2007) and MAGUKs for glutamate receptors (Elias and Nicoll, 2007).

Besides the role of intracellular protein scaffolds, a few systems have been suggested to control the synaptic localization of neurotransmitter receptors through extracellular interactions (see Gerrow and El-Husseini, 2007). For example, the ectodomain of the NMDA receptor (NMDAR) was reported to interact physically with the ephrin receptor EphB2 in the presence of EphrinB, resulting in NMDAR clustering (Dalva *et al*, 2000) and enhanced NMDAR-dependent calcium entry (Takasu *et al*, 2002). Yet, disruption of *EphB2* in mutant mice causes a reduction but not a disappearance of NMDAR synaptic clusters (Henderson *et al*, 2001), indicating the contribution of parallel systems for NMDAR localization at synapses. Similarly, the neuronal pentraxin 1 (NP1) (Schlimgen *et al*, 1995) and the neuronal activity-regulated pentraxin Narp (Tsui *et al*, 1996) are calcium-dependent lectins that are secreted into the synaptic cleft and localize at glutamatergic synapses. They assemble in multimeric complexes that bind AMPA receptors and trigger their aggregation (O'Brien *et al*, 1999; Xu *et al*, 2003). Yet, the *in vivo* contribution of pentraxins to the localization of AMPA receptors at the synapse is not completely understood. A triple knock-out mouse, in which the three genes encoding NP1, Narp and the transmembrane neuronal pentraxin receptor (NPR) have been inactivated, displays only subtle behavioural defects (Bjartmar *et al*, 2006). In these mice, a decrease of GluR4 containing synapses could be detected in the hippocampus (Sia *et al*, 2007), as well as a block of LTD induced by metabotropic glutamate receptor stimulation at the Schaffer collateral-CA1 synapse (Cho *et al*, 2008). Thus, this extracellular protein–receptor interaction may provide modulatory functions rather than have a central role in the organization of post-synaptic domains.

Results previously obtained at cholinergic NMJs of the nematode *Caenorhabditis elegans* indicate that an extracellular scaffold may have an essential role in the clustering of ionotropic receptors at these synapses (Gally *et al*, 2004; Gendrel *et al*, 2009). In *C. elegans*, both heteromeric and homomeric ionotropic AChRs are present at NMJs. The two types of AChRs can be discriminated by their distinct pharmacological profiles (Richmond *et al*, 1999).

*Corresponding author. Institute of Biology of the Ecole Normale Supérieure, 46 rue d'Ulm, Paris 75005, France. Tel.: +33 14 432 2305; Fax: +33 14 432 3654; E-mail: jlbesse@biologie.ens.fr

Received: 16 June 2010; accepted: 16 December 2010; published online: 21 January 2011

The heteropentameric AChRs are activated by the drug levamisole—a nematode-specific cholinergic agonist that causes muscle hypercontraction and death of wild-type animals at high concentrations (Lewis *et al*, 1980; Fleming *et al*, 1997)—and are inhibited by nicotine (Boulin *et al*, 2008). These levamisole-sensitive AChRs (L-AChRs) are composed of five subunits, including the three α subunits UNC-38, UNC-63 and LEV-8, and the two non-α subunits UNC-29 and LEV-1. The second type of receptor, activated by nicotine and partially blocked by levamisole, is most likely homomeric, composed of ACR-16 subunits (Francis *et al*, 2005; Touroutine *et al*, 2005; Boulin *et al*, 2008). Heteromeric L-AChRs and nicotine-sensitive homomeric AChRs (N-AChRs) are largely redundant *in vivo* as mutants lacking either L- or N-AChRs display mild or no locomotory defect, while absence of both L- and N-AChRs cause almost complete paralysis of the animals.

Intriguingly, distinct machineries have evolved to localize these two types of AChRs at the *C. elegans* NMJ. Proper synaptic localization of ACR-16 requires CAM-1, a Ror receptor tyrosine kinase. In *cam-1* mutants, an ACR-16-GFP fusion protein appears mis-localized and N-AChR-dependent currents are absent, while L-AChRs are functional and properly localized at the synapse (Francis *et al*, 2005). Conversely, L-AChR clustering but not N-AChR clustering specifically requires the transmembrane protein LEV-10 and the secreted protein LEV-9 (Gally *et al*, 2004; Gendrel *et al*, 2009). In *lev-9* or *lev-10* mutant animals, L-AChRs are properly expressed, trafficked to the muscle plasma membrane and functional but remain diffusely distributed on the muscle cell surface. These mutants present a mild locomotory defect and are more resistant to levamisole than wild-type animals. LEV-9 and LEV-10 are expressed post-synaptically in body-wall muscles and form clusters at NMJs, where they colocalize with L-AChRs. LEV-10 physically interacts with L-AChRs and can directly bind the LEV-9 protein in *ex vivo* assays. This LEV-10 function is mediated by its extracellular domain, specifically the five extracellular CUB (*C*omplement *U*rchin EGF, *B*MP) domains, the single extracellular LDLa domain being dispensable for LEV-10 function (unpublished data). The secreted protein LEV-9 is composed of 8 CCP (complement control protein) domains (also called short complement repeat domains or Sushi domains) and one whey acidic protein (WAP) domain, the latter dispensable for LEV-9 function. Interestingly, the synaptic localization of LEV-9 and LEV-10 requires the expression of L-AChRs as in mutants lacking L-AChRs, LEV-9 and LEV-10 are expressed but no longer cluster at NMJs. Thus, L-AChRs, LEV-9 and LEV-10 form a macromolecular complex in the synaptic cleft of the *C. elegans* NMJs required to localize a specific subtype of AChRs. Yet, the determinants required to nucleate or stabilize this complex at the synapse remain uncharacterized.

To identify additional components of this extracellular synaptic scaffold, we screened for mutants sharing the partial levamisole-resistance phenotype of *lev-9* and *lev-10* mutant animals. Here, we demonstrate that *oig-4* is required for the proper synaptic localization of the L-AChR complex. It encodes a secreted protein with a single immunoglobulin (Ig) domain that forms clusters at NMJs. OIG-4 physically interacts with L-AChRs and LEV-10 and is necessary to stabilize the physical interactions within the L-AChR/LEV-9/LEV-10 complex. Since OIG-4 partially localizes at synapses independently of LEV-9 and LEV-10, it might link the L-AChR-associated complex to local synaptic cues.

Results

oig-4 mutants are partially resistant to the cholinergic agonist levamisole

To identify components required for the synaptic localization of L-AChRs, we screened for mutants that would phenocopy *lev-9* and *lev-10*, two mutants that are defective for L-AChR clustering. When exposed to the cholinergic agonist levamisole, these mutants almost completely paralyse within 2 h (Figure 1A) but subsequently adapt within 12–16 h and recover motility on levamisole concentrations otherwise lethal for wild-type animals (Figure 1B) (Lewis *et al*, 1980; Gally *et al*, 2004; Gendrel *et al*, 2009). We screened EMS-mutagenized worms for recovery of movement after overnight exposure to 1 mM levamisole and isolated the mutant allele *kr39*. A second allele, *kr193*, was isolated in a screen for mutants that failed to complement the *kr39* allele (see Materials and methods). Based on dose–response experiments, the levamisole sensitivity of these two mutants is intermediate between the wild-type and the *lev-9* and *lev-10* mutants when assaying paralysis after both short and prolonged exposure to levamisole (Figure 1A and B). No additional phenotype could be identified.

The mutated locus was identified using classical two-factor genetic mapping, SNP mapping and rescue experiments with fosmids and PCR fragments. The decreased sensitivity to levamisole of *kr39* and *kr193* mutants was rescued by providing a 2.3-kb genomic fragment encompassing the

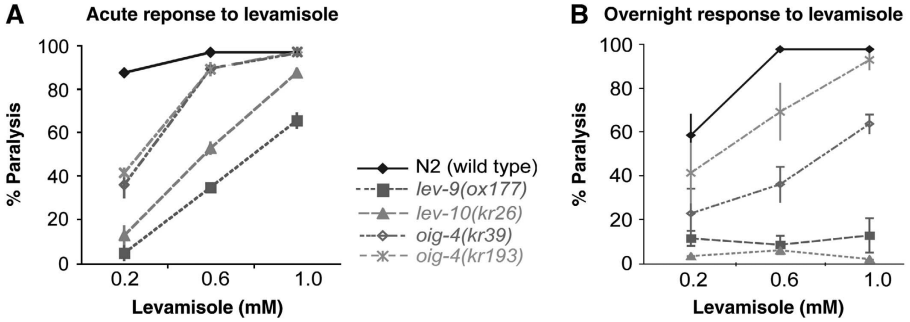

Figure 1 *oig-4* mutant alleles confer partial resistance to levamisole. (**A**) *oig-4*, *lev-10 and lev-9* mutants paralyse after 2 h exposure to levamisole but at higher concentrations than the wild-type (WT) animals. (**B**) After overnight exposure to the drug they regain motility in contrast to the WT (right graph) (mean ± s.e.m., $n = 3$ independent experiments, total number of animals tested per point: 300).

oig-4 coding region surrounded by 1.1 kb upstream and 0.4 kb downstream to the ORF (Figure 2C). Sequencing the *oig-4* genomic locus in *kr39* identified a G to A missense point mutation introducing a glycine to arginine substitution (Figure 2A). The *kr193* mutant contains a G to A point mutation in the fifth base of the splicing donor site of the first *oig-4* intron (Figure 2A). Finally, a deletion allele *oig-4(tm3753)* was isolated by the Japanese *C. elegans* knock-out consortium (Figure 2A). This deletion is predicted to result in an ORF shift affecting the C-terminal part of the protein. *tm3753/kr39* trans-heterozygous animals were slightly less resistant to levamisole than *oig-4(kr39)* homozygous animals ($51 \pm 22\%$ $n = 220$ of *tm3753/kr39* animals and $23 \pm 8\%$ $n = 60$ of *kr39/kr39* animals, remained paralysed after overnight exposure to 0.6 mM levamisole, compared with $99 \pm 2\%$, $n = 60$ animals in the wild type, 3 independent experiments). However, *oig-4(tm3753)* homozygous animals died at early embryonic stages. This lethality could not be rescued when providing a fosmid or PCR fragments containing the *oig-4* genomic locus (data not shown), suggesting that the *oig-4(tm3753)* deletion is closely linked to a second lethal mutation which we could not separate despite extensive outcrossing.

Altogether, these results identify *oig-4* as a new gene required for normal levamisole sensitivity in *C. elegans.*

oig-4 encodes a single Ig-domain-containing protein predominantly expressed in body-wall muscle

oig-4 was initially named *oig* because it is predicted to encode a *o*ne *i*mmunoglobulin-domain protein. To confirm the genome annotations, we isolated a complete *oig-4* cDNA clone. The *oig-4* mRNA is trans-spliced to the Splice Leader SL1, 84 bases upstream of the start codon and there is no evidence of alternative splicing of the coding exons (Figure 2A). *oig-4* encodes a predicted 155 amino-acid secreted protein containing a signal peptide followed by one Ig domain of 72 amino acids (SMART analysis) (Figure 2B). *oig-4* orthologues are detected in the genomes of parasitic and non-parasitic nematodes and in insects including *Drosophila melanogaster* (Supplementary Figure S2). No obvious *oig-4* orthologue is detected outside of the ecdysozoan phylum, although genes coding for proteins with extracellular Ig domains related to OIG-4 can be identified in mammalian genomes.

To characterize the *oig-4* expression pattern, we built a bicistronic vector containing an *oig-4* rescuing genomic fragment and the GFP-coding sequence preceded by a SL2 splice leader acceptor site. This construct drives the expression of *oig-4* and *gfp* in the same cells under the control of *oig-4* regulatory sequences. Providing this construct in *oig-4* mutants rescued levamisole resistance (Figure 2C). GFP was expressed predominantly in body-wall muscle cells

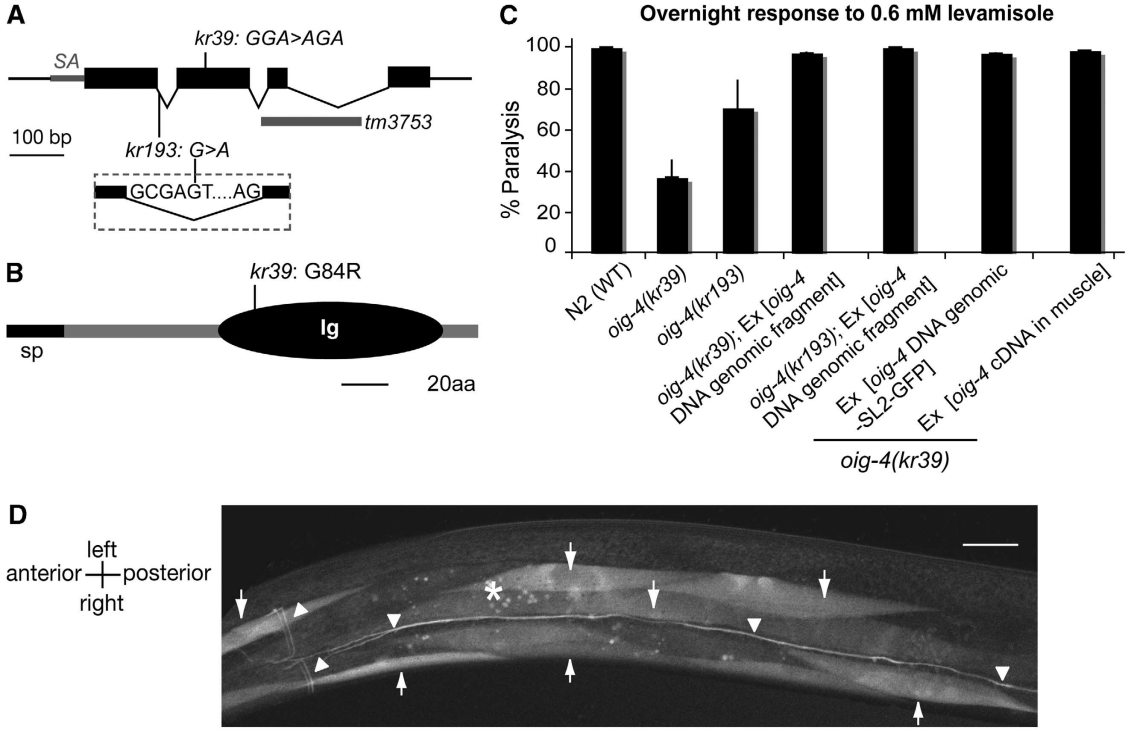

Figure 2 *oig-4* encodes a single immunoglobulin (Ig)-domain protein expressed predominantly in body-wall muscle. (**A**) Structure of the *oig-4* genomic locus. Grey line: 5′ untranslated region, SA: splice acceptor site, black box: coding regions, vertical black lines: point mutations, grey box: deletion. *kr39* is a missense mutation, *kr193* is a change of the fifth base pair of the first intron of *oig-4*, the *tm3753* is a deletion of 239 base pairs. (**B**) OIG-4 is predicted to be a secreted protein. It contains a signal peptide (sp) and one immunoglobulin domain (Ig). The mutation in the *kr39* mutant allele (vertical line) causes a glycine to arginine amino-acid change (G84R). (**C**) An *oig-4* genomic fragment or an *oig-4* cDNA expressed by muscle can rescue the *oig-4* mutant phenotype. Graphs represent the percentage of dead animals after overnight exposure to levamisole 0.6 mM (mean ± s.e.m., $n = 3$ independent experiments of 3–5 independent lines, total number of animals tested: 187–300). (**D**) *oig-4* is expressed predominantly in body-wall muscles (BWM). An artificial operon containing the *gfp* sequence under the control of an *oig-4* genomic fragment drives GFP expression in BWM (arrows). Arrowheads indicate two processes emanating from a pair of head neurons. Non-specific fluorescence is due to the autofluorescence of the intestine (asterisk). Scale bar = 10 μm.

(Figure 2D). GFP was also detected in the pharyngeal muscle cell pm6 and in 4 head neurons, two of which send processes along the ventral nerve cord.

The partial resistance of *oig-4* mutants to levamisole suggested that OIG-4 might regulate the function of L-AChR expressed in the muscle cells. To test whether *oig-4* expression in muscle was sufficient for its function, we expressed an *oig-4* cDNA under the control of the body-wall muscle-specific promoter *Pmyo-3*. Resistance to levamisole was rescued in transgenic *oig-4* mutants (Figure 2C), indicating that muscle expression of *oig-4* is sufficient for its function.

OIG-4 is a secreted protein that clusters at cholinergic NMJs

OIG-4 is predicted to be secreted. To test this hypothesis, we fused GFP to the N-terminus of OIG-4 immediately after the signal peptide and expressed it under the *oig-4* promoter or the muscle-specific promoter *Pmyo-3*. Both constructs rescued the *oig-4(kr39)* mutant phenotype, demonstrating that GFP-OIG-4 was functional (Figure 3A). When GFP is secreted from *C. elegans* body-wall muscle, it is endocytosed and concentrated in coelomocytes, six scavenger cells that filter the fluid of the pseudocoelomic cavity (Fares and Greenwald, 2001). In *Pmyo-3::gfp-oig-4* transgenic animals, GFP-OIG-4 was readily detected in coelomocytes (Figure 3B), thus demonstrating that the OIG-4 protein is effectively secreted from body-wall muscle cells.

The distribution of GFP-OIG-4 was analysed at the subcellular level in *oig-4(kr39)* mutants containing an integrated transgene expressing GFP-OIG-4 under the control of the *oig-4* promoter. These transgenic mutants showed wild-type sensitivity to levamisole (Figure 3A). As GFP fluorescence was barely detectable by light microscopy, we performed immunofluorescence staining using anti-GFP antibodies. GFP-OIG-4 was detected in puncta distributed along the ventral and dorsal nerve cords and in the nerve ring where head muscles are innervated (Figure 3C). These puncta were juxtaposed to cholinergic varicosities stained with antibodies against the vesicular ACh transporter UNC-17 and colocalized with L-AChR clusters (Figure 3C).

Together, these results indicate that OIG-4 is a protein secreted by muscle cells, which clusters post-synaptically at cholinergic NMJs.

oig-4(kr39) is predicted to be a functionally null allele

Deciphering the function of *oig-4* would require a complete loss-of-function allele. The *oig-4(kr193)* mutation affects the first splice donor site at the fifth position, which was demonstrated to be highly conserved (Sheth *et al*, 2006). As predicted, the majority of the *oig-4* mRNA in *kr193* was abnormally retaining the first intron, but 10% of the fully spliced wild-type mRNA remained (Supplementary Figure S1), suggesting that *oig-4(kr193)* is a hypomorphic allele.

The *oig-4(kr39)* allele contains only a missense mutation but displays the strongest mutant phenotype of all three *oig-4* alleles. It behaves as a genetic null allele as animals that are heterozygous for *oig-4(kr39)* and a deficiency of the region show no stronger mutant phenotypes than the *oig-4(kr39)* homozygous mutants. *oig-4(kr39/mnDf99)* are less resistant than *oig-4(kr39/kr39)* after overnight exposure to 0.6 mM levamisole ($31.9 \pm 0.9\%$ and $96.9 \pm 0.9\%$, respectively, $n = 2$ independent experiments, 80 animals per genotype, mean ± s.d.), suggesting that haplo-insufficiency of genes deleted by the deficiency sensitizes the animals to levamisole. To bypass non-specific morbidity that might interfere with the levamisole-resistance phenotype, we analysed L-AChR expression in *oig-4(kr39)* and *oig-4(kr39/mnDf99)* populations by scoring the number of individuals, in which UNC-63-YFP clusters were detectable (see below) and saw no difference between the two genotypes ($18.9 \pm 1.2\%$ and $22.8 \pm 5.5\%$, respectively; $n = 2$ independent experiments, 87–100 animals per genotype). To better characterize the mutant protein synthesized in *oig-4(kr39)* animals, we introduced the G84R mutation in GFP-OIG-4. The mutant protein expressed under the control of the *Pmyo-3* promoter was unable to rescue *oig-4(kr39)* mutants (Figure 3A). By immunofluorescence staining, GFP-OIG-4(G84R) was detected in intracellular compartments of body-wall muscle cells and was absent from NMJs (Figure 3D) and coelomocytes (data not shown). These data suggest that the G84R amino-acid change causes the intracellular retention of the OIG-4 protein, likely due to its abnormal folding. Based on genetic and cellular criteria, *oig-4(kr39)* is, therefore, likely to be a functionally null allele.

OIG-4 is required for proper synaptic localization of L-AChRs

The partial resistance of the *oig-4* mutants to levamisole suggests that disrupting *oig-4* impairs L-AChR function. To characterize L-AChR expression, we performed immunostaining of the L-AChR subunit UNC-38. In the wild type, UNC-38 forms clusters in the ventral and the dorsal cord. In most *oig-4* mutants, UNC-38 was no longer detectable (Figure 4A), while pre-synaptic cholinergic boutons were wild type based on staining of the vesicular ACh transporter UNC-17. Similar data were obtained for the L-AChR subunit UNC-29 (data not shown). In wild-type animals, L-AChRs colocalize with the ACR-16-containing N-AChRs (Gendrel *et al*, 2009). Based on immunofluorescence staining, N-AChRs were properly clustered at NMJs in *oig-4* mutants, suggesting proper differentiation of cholinergic synapses (Figure 4A). Finally, the distribution of the muscle $GABA_A$ receptor UNC-49 present at inhibitory NMJs was undistinguishable between *oig-4* mutants and wild-type animals (Figure 4A). Therefore, disruption of the *oig-4* gene specifically affects the localization of L-AChRs at the synapses, independently of NMJ formation.

Although prominent, the loss of L-AChRs was not fully penetrant in *oig-4* mutant animals; residual staining of the L-AChR subunit UNC-38 could be detected by immunofluorescence, in a subset of *oig-4* mutant animals (see Figure 7B). To quantify this phenotype we used the L-AChR subunit knock-in UNC-63-YFP (Gendrel *et al*, 2009). In this strain L-AChRs can be visualized in living animals, which circumvents the technical issues encountered in immunofluorescence experiments due to variable permeabilization of the worms. L-AChR clusters were absent in 80% of *oig-4(kr39)* animals, while in the remaining 20% of the population UNC-63-YFP puncta were detected, although they appeared smaller than in most wild-type animals (100 animals, 3 independent experiments) (Figure 4B and C).

The decreased synaptic localization of L-AChRs could reflect an overall decrease of L-AChR expression level, as in *unc-50* mutants, or a redistribution in the plasma membrane, as in *lev-9* and *lev-10* mutants (Eimer *et al*, 2007). Western blot analysis of L-AChR subunit UNC-29 expression indicated

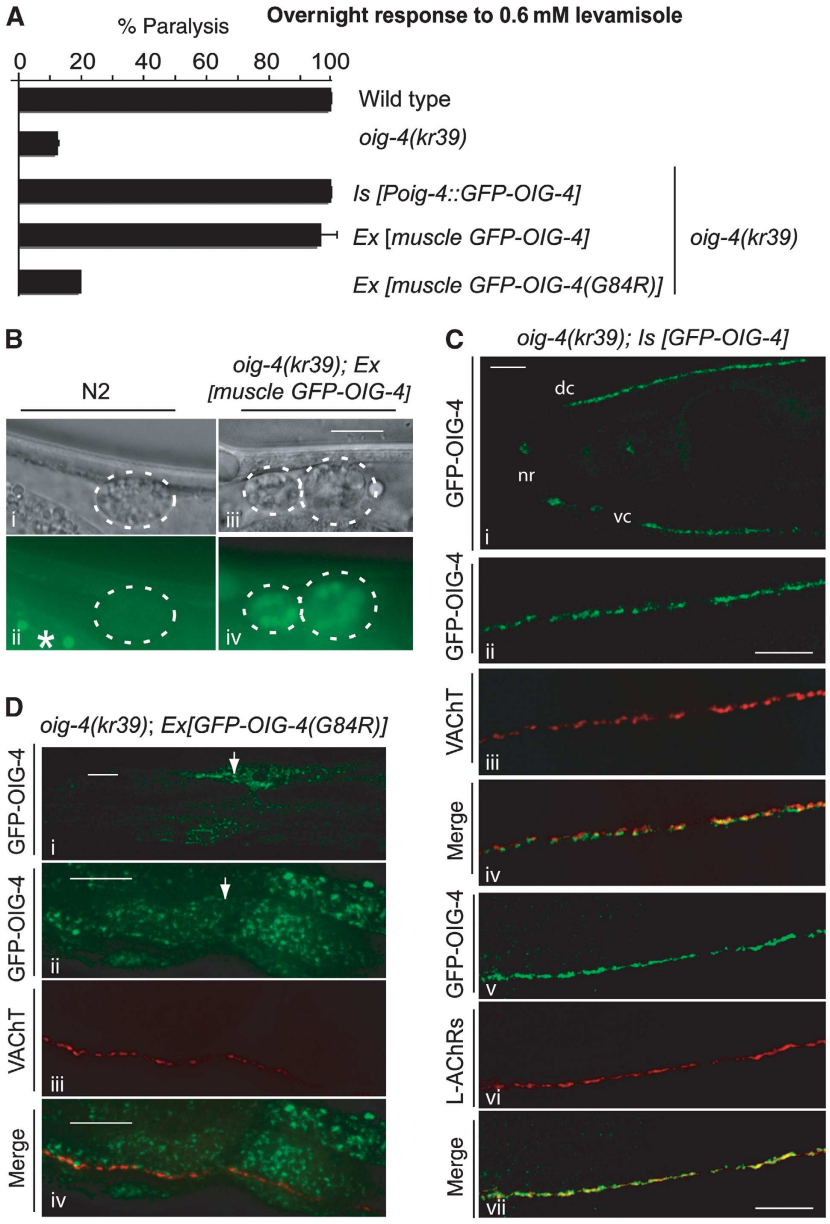

Figure 3 OIG-4 is secreted and clustered at neuromuscular junctions (NMJs) while the mutated protein GFP-OIG-4(G84R) is retained intracellularly. (**A**) The GFP-OIG-4 translational fusion but not the mutated GFP-OIG-4(G84R) rescues the *oig-4* mutant phenotypes. Graph represents the percentage of dead animals after overnight exposure to levamisole 0.6 mM (mean ± s.e.m., $n = 3$ independent experiments of 3–5 independent lines, total number of animals tested: 100–300). *Ex:* extrachromosomal transgene; *Is*: genome integrated transgene; expression was achieved using the *oig-4* promoter (*Poig-4*) or the muscle-specific promoter *Pmyo-3* (*muscle*). (**B**) GFP-OIG-4 is secreted. The GFP-OIG-4 translational fusion expressed by the muscle promoter *Pmyo-3* in transgenic *oig-4* mutants is detected in coelomocytes. Coelomocytes (dotted circle) are visualized by Nomarski (i, iii) and epifluorescence microscopy (ii, iv) in wild-type (i, ii) and transgenic animals (iii, iv). Asterisk indicates intestine autofluorescence; scale bar = 10 μm. (**C**) GFP-OIG-4 forms clusters at NMJs GFP-OIG-4 were detected in the nerve ring (nr), and in both the dorsal and ventral nerve cords (dc, vc) using anti-GFP immunofluorescence staining (i). GFP-OIG-4 clusters are juxtaposed to the pre-synaptic cholinergic boutons visualized by immunostaining of the vesicular acetylcholine transporter (VAChT) UNC-17 (ii–iv) and colocalize with L-AChR clusters stained by antibodies against the UNC-38 subunit (v–vii). Scale bar = 10 μm. (**D**) GFP-OIG-4(G84R) is retained in the muscle cell bodies (i, ii) and does not reach NMJs visualized by anti-UNC-17 immunostaining (iii). Arrows indicate muscle cells. Scale bar = 10 μm.

that the L-AChR expression level was similar to wild type in *oig-4(kr39)* and *oig-4(kr193)* mutants (104 ± 6% and 134 ± 40% of wild type, respectively, $n = 4$) (Figure 4D). To investigate whether the expressed L-AChRs were properly inserted into the plasma membrane and were functional, we performed an electrophysiological analysis. Pressure-ejection of levamisole on voltage-clamped muscle cells elicited currents similar in *oig-4* null mutants and wild-type animals (Figure 5A and B). Therefore, L-AChRs are properly expressed and functional in *oig-4* mutants but their density at the synapse as measured by immunofluorescence is decreased and becomes undetectable in most mutant animals.

To evaluate the functional population of L-AChRs at the synapses of *oig-4* mutants, we electrically stimulated

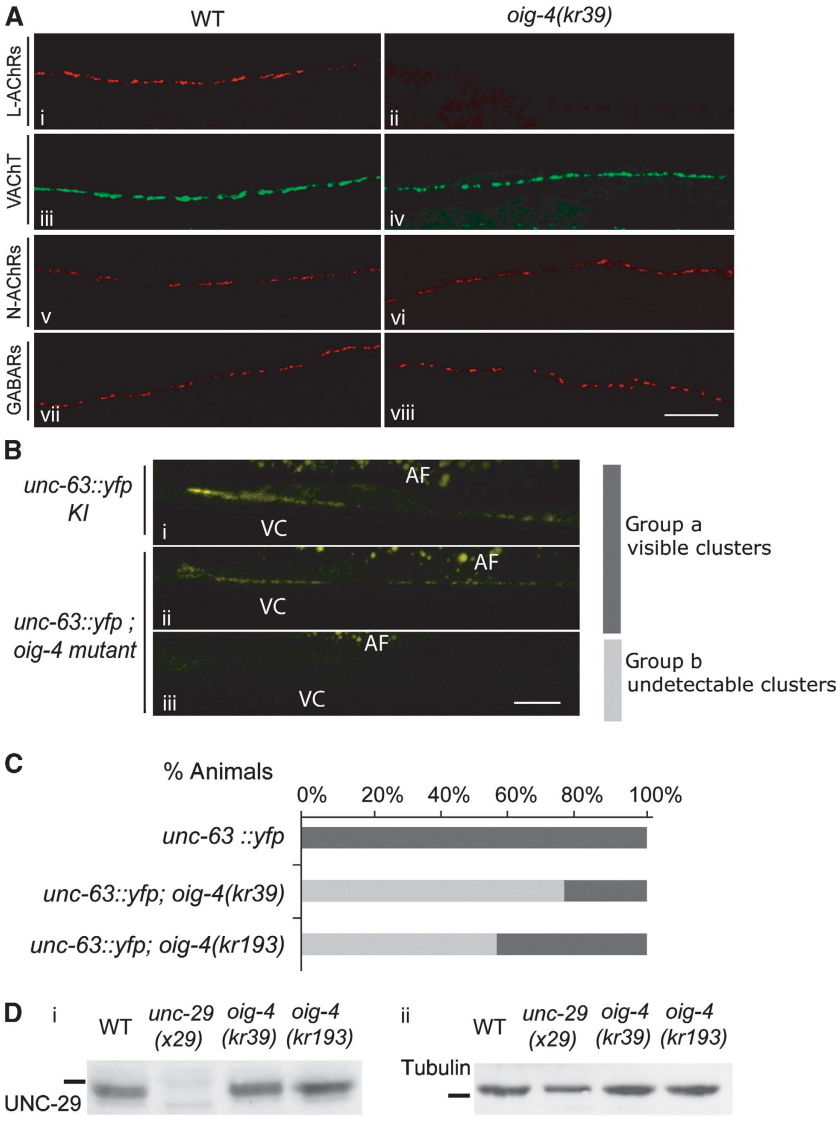

Figure 4 L-AChRs are properly expressed but not detected at the NMJs of *oig-4* mutants. (**A**) The UNC-38 L-AChR subunit cannot be detected by immunostaining at the dorsal cord of *oig-4* mutants (ii) when compared with wild-type (WT) animals (i). The pre-synaptic varicosities in *oig-4* mutants (iv) form properly as in wild type (iii). ACR-16 N-AChR and UNC-49 GABA receptor distribution in *oig-4* mutants (vi, viii) is not affected compared with wild type (v, vii). Scale bar = 10 μm. (**B**) Distribution of the knocked-in UNC-63-YFP L-AChR subunit scored *in vivo* in *oig-4* mutant populations. In the reference knock-in strain (i) UNC-63-YFP is detected in ventral (VC) nerve cord and dorsal nerve cord (not shown). In the *oig-4* mutant background UNC-63-YFP is either still detected as weak clusters (ii, group a) or not clustered in the cords (iii, group b) (AF: autofluorescence from intestine). Scale bar = 10 μm. (**C**) Quantification of groups a and b (see **B**) in WT and *oig-4* mutant background. The graph represents results of two independent experiments after blind scoring of 100 animals per experiment for each genotype. (**D**) Western blot analysis of UNC-29 L-AChR subunit expression. UNC-29 levels were normalized to tubulin A. (Percentage of wild-type levels in the *oig-4(kr39)* and *oig-4(kr193)* was 104 ± 6% ($n = 4$) and 134 ± 40% ($n = 4$), respectively, mean ± s.d.) Bar indicates the 50 kDa marker.

motoneurons in the ventral cord and recorded evoked currents in individual muscle cells. This analysis was performed in an *acr-16; unc-49* double mutant background to eliminate currents due to the activation of N-AChRs and GABA receptors. In *unc-49; acr-16; oig-4* triple mutants, the time-to-peak and decay time of the evoked currents were significantly increased when compared with *unc-49; acr-16* (Figure 5C, E, F). Such broadened responses are reminiscent of previous observations in *lev-9* and *lev-10* mutants and can be explained by a diffuse distribution of the receptors in the post-synaptic plasma membrane. To our surprise, however, the size of the L-AChR-dependent evoked responses of *oig-4* mutants was similar to the wild type (Figure 5D), in contrast to the reduced evoked amplitudes observed in *lev-9* and *lev-10* mutants (Gally *et al*, 2004; Gendrel *et al*, 2009). Altogether, these data indicate that OIG-4 is required for proper clustering of L-AChRs at NMJs, but functionally differs from the previously characterized L-AChR clustering proteins LEV-9 and LEV-10.

OIG-4 is required for the proper synaptic localization of LEV-9 and LEV-10 proteins

The clustering of L-AChRs was previously demonstrated to rely on physical interactions between the L-AChR, LEV-9 and LEV-10 proteins forming a tripartite complex which is recruited to or stabilized at the synapse (Gally *et al*, 2004; Gendrel *et al*, 2009). To investigate possible cross-talk

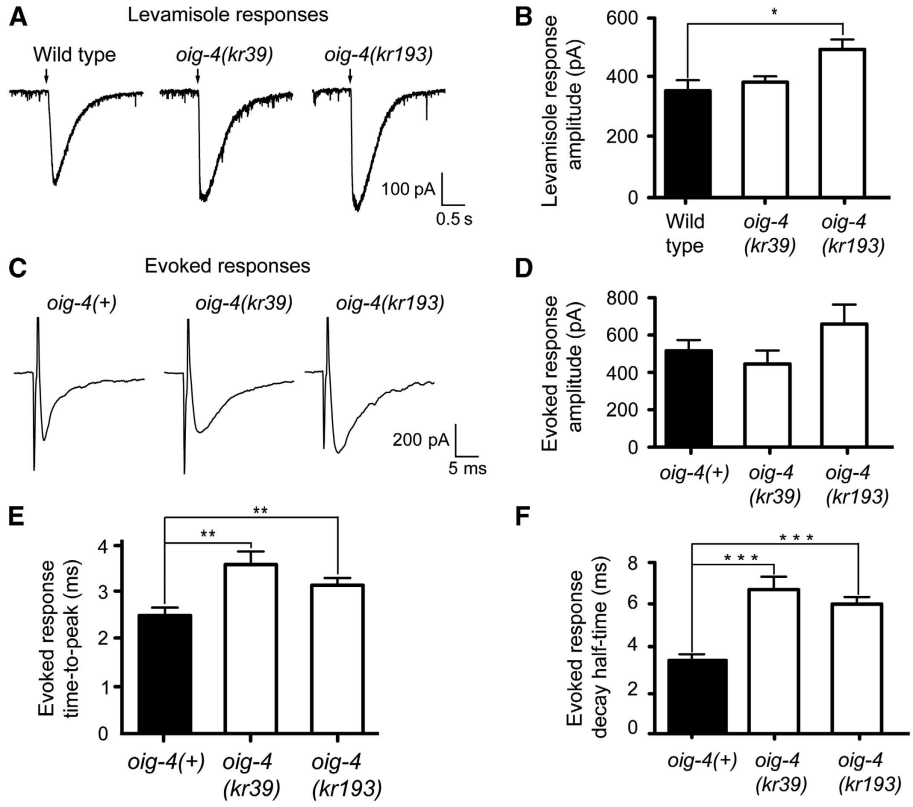

Figure 5 L-AChRs are functional but diffusely distributed at the muscle membrane of *oig-4* mutants. (**A**, **B**) L-AChRs are functional in *oig-4* mutants. Response to pressure ejection of levamisole in voltage-clamped ventral muscle cells. Black arrows mark the 100 ms application onset for 5×10^{-4} M levamisole. The graph indicates the mean ± s.e.m. of the levamisole-elicited current amplitude (366.7 ± 36.6 for N2, $n = 7$; 393.7 ± 20.1 for *oig-4(kr39)*, $n = 6$, $P = 0.1605$; 509.4 ± 34.0 for *oig-4(kr193)*, $n = 7$, $P = 0.0175$). (**C**–**F**) Evoked currents recorded from body-wall muscles after ventral nerve cord stimulation. (**D**) Evoked response amplitudes are 515.9 ± 57.90 for *oig-4(+)*, $n = 14$ versus 445.0 ± 72.76 for *oig-4(kr39)*, $n = 7$ and 659.2 ± 104.5 for *oig-4(kr193)*, $n = 11$. The evoked response time-to-peak (**E**) and decay half-time (**F**) are increased in *oig-4* mutants as compared to wild type (time-to-peak: 1.58 ± 0.14 ms, $n = 13$ for *oig-4(+)* versus 2.53 ± 0.20 ms, $P = 0.0053$, $n = 7$ in *oig-4(kr39)* background, and 2.09 ± 0.11 ms, $P = 0.0051$, $n = 10$ in *oig-4(k193)* background). Decay half-time: 3.45 ± 0.22, $n = 15$ for wild type and 6.49 ± 0.55 ms, $P = 0.0007$, $n = 8$ for *oig-4(kr39)* and 6.07 ± 0.35 ms, $P = 0.0002$, $n = 11$ for *oig-4(kr193)*. Electrically evoked responses were obtained in an *unc-49(e407);acr-16(ok789)* background to eliminate currents due to GABAR and N-AChR activation. $^{*}P < 0.05$, $^{**}P < 0.01$, $^{***}P < 0.001$. Error bars are s.e.m.

between OIG-4 and this machinery we analysed the distribution of LEV-9 and LEV-10 in *oig-4* mutants. In most *oig-4(kr39)* mutants, LEV-9 and LEV-10 were no longer detected at the nerve cords by immunostaining, in contrast to wild-type animals where both proteins were clustered at NMJs (Figure 6A and B). However, LEV-10 was still expressed at levels similar to the wild type based on western blot analysis of fractionated worm extracts (Figure 6C). The LEV-9 protein was barely detectable by immunoprecipitation (IP) in *oig-4* mutant extracts (Figure 6D). These results are very similar to observations in mutants lacking L-AchRs, in which LEV-10 remains expressed but no longer clusters at the synapse and LEV-9 is degraded after being secreted by muscle cells (Gendrel *et al*, 2009). The low levels of LEV-9 protein remaining detectable by IP in *oig-4* mutants likely correspond to the small remaining clusters of LEV-9 detected by immunofluorescence in <10% of animals (Figure 7).

To test whether the proteins of the L-AChR/LEV-9/LEV-10 complex can still associate in the absence of OIG-4, we analysed the relative distribution of these components in the rare *oig-4* mutant animals that retain detectable L-AChR clusters. Based on co-immunostaining experiments LEV-9 colocalized with the residual L-AChR clusters (Figure 7A) and the small detectable LEV-10 puncta were associated with residual LEV-9 staining (Figure 7B). The remaining L-AChR clusters in *oig-4* mutants still colocalized with ACR-16 (data not shown). Therefore, in the absence of OIG-4, L-AChRs, LEV-9 and LEV-10 likely retain the ability to associate at the synapse although their proper localization is highly disturbed.

To dissect the genetic interactions between *oig-4*, *lev-9* and *lev-10* we built a combination of double mutants and analysed the *in vivo* localization of the UNC-63-YFP knock-in subunit. Small clusters could be detected in the ventral or dorsal cord in 24% of *oig-4(kr39)* mutants, whereas UNC-63-YFP clusters were undetectable in *oig-4; lev-10* or *oig-4; lev-9* double mutants ($n = 50$ animals per genotype, two independent experiments, data not shown). Hence, the LEV-9 and LEV-10 proteins are necessary for L-AChR clustering in the presence or absence of OIG-4.

The synaptic localization of OIG-4 is partially independent of LEV-9 and LEV-10

We previously demonstrated that disrupting any of the proteins of the L-AChR/LEV-9/LEV-10 complex causes a loss of synaptic clustering of the remaining partners, suggesting that additional components are required to stabilize the complex at the synapse. To test if OIG-4 can localize at the synapse

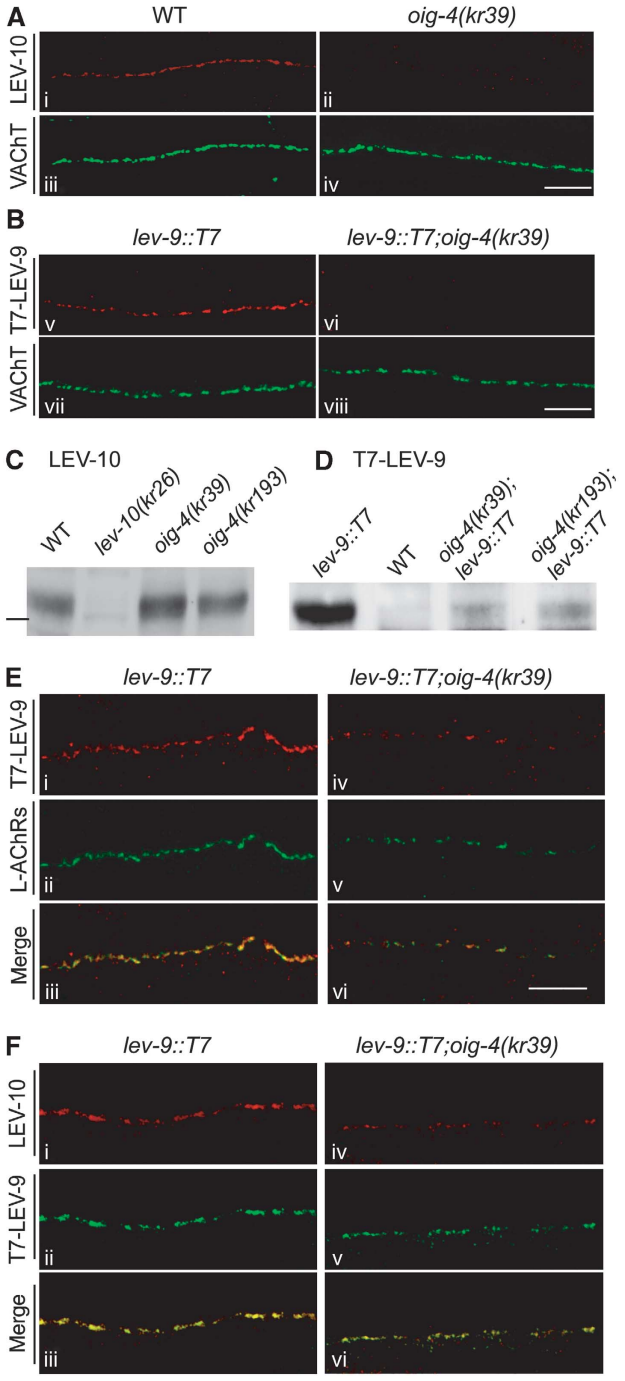

Figure 6 LEV-10 and LEV-9 are not properly localized at the neuromuscular junctions of most *oig-4* mutants. (**A**) Immunostaining of LEV-10 at the dorsal cord of WT and *oig-4* mutants. (**B**) Detection of the knocked-in T7-LEV-9 protein using anti-T7 immunostaining. Scale bar = 10 μm. (**C**) Western blot analysis of LEV-10 expression normalized to total protein content. (Percentage of wild-type levels in the *oig-4(kr39)* and *oig-4(kr193)* was 87 ± 7% ($n = 4$) and 114 ± 24% ($n = 4$) respectively, mean ± s.d.) Bar indicates the 100 kDa marker. (**D**) The T7-LEV-9 protein immunoprecipitated from total worm extracts is weakly detected in *oig-4* mutants. (**E**) Weak L-AChR clusters can be detected by immunostaining in rare *oig-4(kr39)* mutant animals (v) and colocalize with remaining LEV-9-T7 clusters (iv–vi). (**F**) The weak clusters of T7-LEV-9 infrequently detected in *oig-4(kr39)* mutants (v), colocalize with remaining staining of the LEV-10 protein (iv–vi). Scale bar = 10 μm.

independently of L-AChRs, LEV-9 and LEV-10, we analysed GFP-OIG-4 localization in *unc-29(x29)*, *lev-10(kr26)* and *lev-9(ox177)* null mutants using anti-GFP immunostaining to increase detection sensitivity. The GFP-OIG-4 protein was undetectable at NMJs in animals that did not express the L-AChR subunit UNC-29 (Figure 7A). However, GFP-OIG-4 remained expressed at wild-type levels based on western blot analysis and was normally secreted based on GFP detection in coelomocytes (Figure 7B and C). By contrast, GFP-OIG-4 clusters were observed along the nerve cords of *lev-10(kr26)* and *lev-9(ox177)* null mutants (Figure 7A). However, these clusters were detected in only about half of the mutant animals (46 ± 17% and 44 ± 9%, respectively; $n = 2$ experiments, 81–84 animals per genotype) and were smaller and more sparse than in the wild type. To test if these remaining clusters were at synapses, we performed double immunostaining using anti-UNC-17 antibodies, to visualize the presynaptic sites of NMJs. Residual OIG-4 clusters juxtaposed to the UNC-17 vesicular ACh transporter, in the absence of LEV-9 or LEV-10, as in the wild-type background.

These results indicate that OIG-4 absolutely requires L-AChRs to localize at the synapse. However, it can interact with synaptic determinants independently of LEV-9 and LEV-10, possibly in association with the 10–20% of L-AChRs that were estimated to remain near the synapse in *lev-9* and *lev-10* mutants based on previous electrophysiological analysis (Gally *et al*, 2004; Gendrel *et al*, 2009).

OIG-4 interacts in a physical complex with L-AChRs and LEV-10 and stabilizes the L-AChR/LEV-10 interaction

OIG-4 is a secreted synaptic protein, which depends on L-AChRs for its synaptic localization and regulates the presence of the L-AChR/LEV-9/LEV-10 complex at NMJs. To test if OIG-4 may physically interact with this extracellular synaptic scaffold, we performed IP experiments using *oig-4(kr39)* mutants rescued by an integrated transgene driving the expression of GFP-OIG-4. The L-AChR subunit UNC-29 and the LEV-10 protein were co-immunoprecipitated with GFP-OIG-4 from fractionated worm extracts of transgenic mutants but not of wild-type animals using anti-GFP antibodies (Figure 8A and B). Thus, the OIG-4 protein interacts *in vivo* in a stable complex with L-AChRs and LEV-10. To test if OIG-4 can engage stable interactions with L-AChRs or LEV-10 independently of the formation of the L-AChR/LEV-9/LEV-10 complex, we performed similar experiments in *unc-29* and *lev-10* mutant strains. We observed that OIG-4 and UNC-29 no longer co-immunoprecipitate in the absence of LEV-10. Similarly, OIG-4 and LEV-10 no longer co-immunoprecipitate in the absence of UNC-29. These results suggest that cooperative interactions occur within the L-AChR-associated macromolecular complex and likely stabilize the interaction between OIG-4 and L-AChRs.

As described in the previous sections, the loss of OIG-4 causes a redistribution of L-AChRs and its associated partners. We showed that LEV-9 is unstable and degraded in *oig-4* mutants. However, LEV-10 is still expressed at wild-type levels and might remain associated with diffusely distributed L-AChRs. Alternatively, the L-AChR/LEV-10 interaction might only be stable in a macromolecular complex involving OIG-4. To test these hypotheses, we immunoprecipitated UNC-63-YFP from *unc-63-yfp* knock-in strain protein extracts using anti-GFP antibodies. In the wild type, LEV-10 co-immunopre-

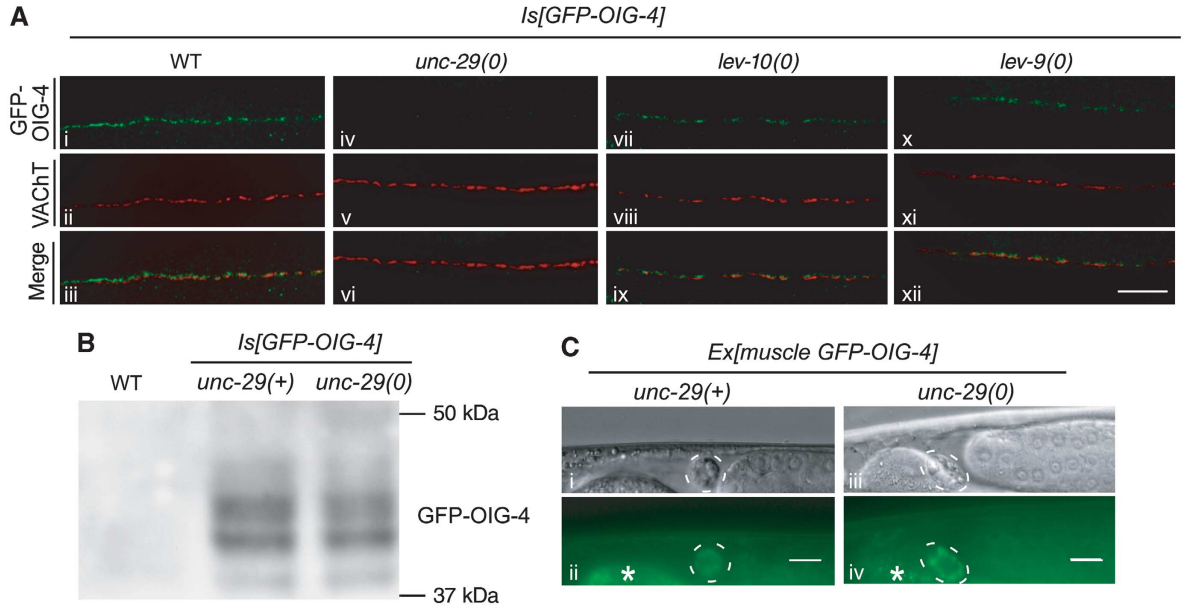

Figure 7 The synaptic localization of GFP-OIG-4 requires L-AChRs while LEV-10 and LEV-9 are partially dispensable. (**A**) GFP-OIG-4 is no longer clustered in the *unc-29(x29)* null mutant background (iv). However, small clusters of GFP-OIG-4 can be detected in *lev-10(kr26)* and *lev-9(ox177)* null mutants. Pre-synaptic VAChT is labelled using anti-UNC-17 antibodies. Scale bar = 10 μm. (**B**) Western blot analysis of GFP-OIG-4 expression in the *unc-29* mutant background (percentage of the wild-type GFP-OIG-4 levels in the *unc-29* mutant background was 78.3 ± 10.8% (mean ± s.d., $n = 3$)). (**C**) GFP-OIG-4 expressed in muscle cells under the control of the *Pmyo-3* promoter is still secreted and accumulates in coelomocytes of WT and *unc-29* null mutants. A wild type-like GFP-OIG-4 translational fusion expressed by the muscle promoter *Pmyo-3* in transgenic *oig-4;unc-29* mutants is detected in coelomocytes. Coelomocytes (dotted circle) are visualized by Nomarski (i, iii) and epifluorescence microscopy (ii, iv) in *unc-29(+)* (i, ii) and *unc-29* null mutant background (iii, iv). Asterisk indicates autofluorescence of intestine. Scale bar = 10 μm.

cipitates with UNC-63-YFP (Gendrel *et al*, 2009). In an *oig-4(kr39)* background, we observed that LEV-10 no longer co-immunoprecipitated with UNC-63-YFP (Figure 8C). These results indicate that OIG-4 directly or indirectly stabilizes the L-AChR/LEV-10 interaction.

Discussion

A genetic screen for mutants partially resistant to the cholinergic agonist levamisole identified *oig-4*, a gene coding for a small extracellular protein containing a single Ig domain. This protein is secreted by muscle cells and is required for the synaptic localization of L-AChRs at the NMJ. OIG-4 is engaged in a physical complex containing L-AChRs and two additional proteins, LEV-9 and LEV-10, previously demonstrated to associate in the synaptic cleft for L-AChR clustering. While each component of the L-AChR/LEV-9/LEV-10 complex strictly depends on its partners for its synaptic localization, OIG-4 remains partially synaptically localized in the absence of LEV-9 or LEV-10, suggesting that it may bind other synaptic determinants and thereby anchor the L-AChR/LEV-9/LEV-10 at the NMJ.

A novel synaptic function for a member of the Ig super family (IgSF)

Predicted orthologues of OIG-4 are readily detected in different genera of parasitic and non-parasitic nematodes such as *Brugia malayi* and *Pristionchus pacificus* (see Supplementary Figure S2). In addition the genome of *C. elegans* contains a clear paralogue of *oig-4*, *oig-1*, which remains uncharacterized so far (see Supplementary Figure S2). Orthologues of OIG-4 are also detected in insects, but none of these genes has a characterized function. Interestingly, a screen for genes whose overexpression caused anatomical defects of *Drosophila* NMJs tentatively identified the *oig-4* orthologue CG14141 (Kraut *et al*, 2001). However, this result remains inconclusive, as the transposon used to achieve CG14141 overexpression might have affected the expression of nearby loci and detailed analysis of CG14141 specifically was not performed to our knowledge. As clear orthologues of *lev-9* and *lev-10* are also present in ecdysozoan genomes, it is tempting to speculate that the function of OIG-4 has been conserved through the evolution of ecdysozoans, cooperating with LEV-9 and LEV-10 orthologues to localize ionotropic neurotransmitter receptors. In mammals, the best studied secreted protein single Ig-domain protein, β2-microglobulin, non-covalently associates with a transmembrane subunit containing three Ig domains to form class I molecules of the major histocompatibility complex (Rammensee *et al*, 1993). Databases also contain transcripts that are predicted to encode small secreted single Ig proteins arising from neuronal genes encoding the transmembrane receptors Robo2 or Ror1. However, the products of these transcript variants have not been functionally validated.

Ig domains are among the most abundant domains found in extracellular proteins, including some important players involved in synapse formation and maintenance. For example, the Ig-rich transmembrane proteins SYG-1 and SYG-2 specify the synapses made by the HSN serotoninergic neuron in *C. elegans* (Shen and Bargmann, 2003; Shen *et al*, 2004). Basigin, a transmembrane protein containing two Ig domains, localizes pre- and post-synaptically at the *D. melanogaster*

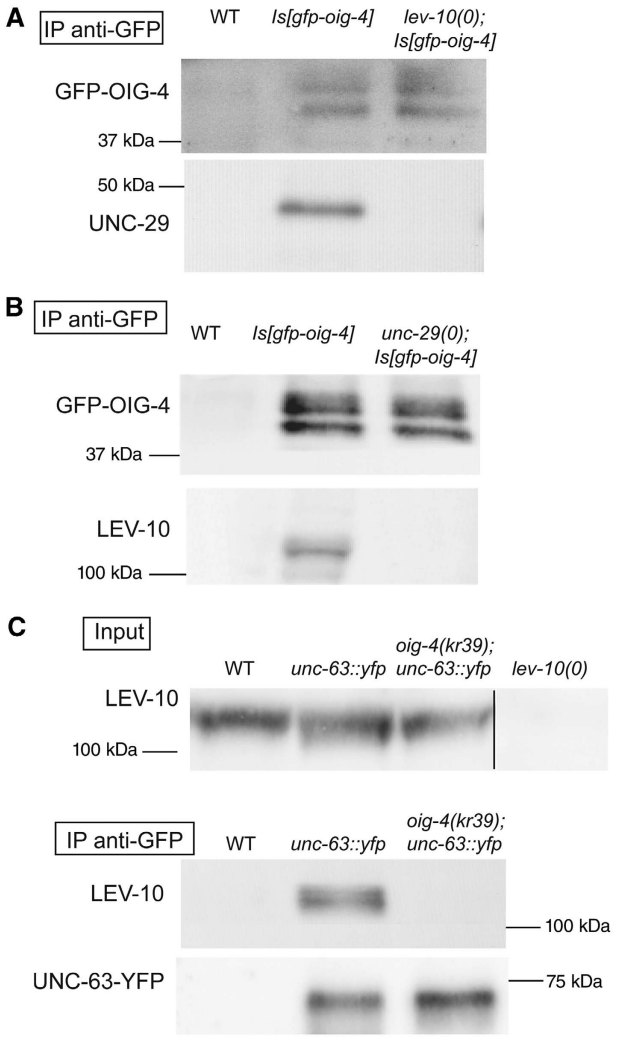

Figure 8 The OIG-4 interacts physically with L-AChRs and LEV-10 and stabilizes the L-AChR/LEV-10 interaction. (**A**) Detection of the UNC-29 L-AChR subunit after immunoprecipitation of GFP-OIG-4 using anti-GFP antibodies from WT and transgenic lines expressing GFP-OIG-4. UNC-29 no longer co-precipitates when GFP-OIG-4 is expressed in a *lev-10(kr26)* null mutant background ($n = 3$ independent experiments). (**B**) LEV-10 co-immunoprecipitates with OIG-4-GFP as above. The interaction is lost in an *unc-29(x29)* null mutant background ($n = 3$ independent experiments). (**C**) LEV-10 is co-immunoprecipitated with UNC-63-YFP using anti-GFP antibodies. Co-precipitation is lost in an *oig-4(kr39)* mutant background ($n = 3$ independent experiments).

NMJ where it regulates several synaptic features including the distribution of synaptic vesicle clusters and neurotransmitter release (Besse *et al*, 2007). In vertebrates, IgSF members regulate neuritic outgrowth, synaptic formation and plasticity (for reviews, see Rougon and Hobert, 2003; Cox *et al*, 2004; Shapiro *et al*, 2007). For example, SynCAMs (synaptic cell adhesion molecules) are transmembrane proteins containing three Ig domains in the extracellular region. Through trans-synaptic homophilic and heterophilic interactions, they can regulate the number of pre-synaptic specializations that form on a neuron (Biederer *et al*, 2002). Similarly, Sidekick-1, -2, Dscam and Dscam-like-1 are expressed in mutually exclusive neurons and control synaptic selectivity in the retina through homophilic interactions (Yamagata *et al*, 2002; Yamagata and Sanes, 2008). Interestingly, all these proteins contain PDZ-binding domains at their C-terminus, which interact with an intracellular post-synaptic scaffold. This interaction can, in turn, stabilize the post-synaptic scaffold and enhance the recruitment of neurotransmitter receptors (Yamagata and Sanes, 2010). OIG-4 adds a novel paradigm for the IgSF family as it is a secreted protein that is required for L-AChR clustering activity solely through extracellular interactions and independently of synapse formation.

OIG-4 differs from the core L-AChR clustering components LEV-9 and LEV-10

The remarkably similar phenotypes shared by *lev-9* and *lev-10* mutants provided the rationale for a screen that would identify additional genes involved in the synaptic clustering of L-AChRs. These mutant animals acutely paralyse when exposed to high concentrations of levamisole but they adapt overnight. In these mutants, L-AChR clusters are no longer detectable at NMJs and electrophysiological measurements reveal a profound decrease in L-AChR-dependent synaptic responses. Our screen for mutants that phenocopy *lev-9(0)* or *lev-10(0)* animals identified a novel gene required for L-AChR clustering, yet *oig-4* differs phenotypically from *lev-9* or *lev-10* mutants. First, *oig-4(kr39)* animals are less resistant to levamisole despite the fact that *kr39* is a functional null mutation based on genetic and biochemical criteria. Second, small L-AChR clusters are retained in about 20% of the mutants. As the *oig-1* paralogue of *oig-4* has not been characterized we cannot rule out a partial redundancy between the two genes that could account for the incomplete penetrance of the *oig-4* phenotype. However, since LEV-9 and LEV-10 are associated with the remaining L-AChR clusters in *oig-4(kr39)*, they likely form a core complex which is recruited or stabilized at the synapse by OIG-4. Third, the most striking difference between *oig-4* and *lev-9* and *lev-10* is the persistence of an evoked synaptic response with wild-type amplitude despite increased time-to-peak and decay time that are consistent with L-AChR declustering.

Several hypotheses could be raised to account for the discrepancy between imaging and electrophysiological data. First, more receptors might remain near Ach release sites in *oig-4* than in *lev-9* and *lev-10* mutants. In *lev-9* and *lev-10* mutants, L-AChRs are not detected by immunofluorescence despite the recording of an evoked response of roughly 20% the wild-type size. The detection of L-AChRs in a significant fraction of the *oig-4* mutants might reflect a less profound decrease of the overall synaptic population of receptors. Yet, the signal-to-noise ratio of our immunofluorescence staining conditions is around 10. Even if the synaptic density of L-AChRs is just below the detection threshold in *oig-4* mutants, it remains difficult to reconcile the wild-type size of the recorded synaptic response, unless small undetectable LEV-9/LEV-10-dependent L-AChR aggregates form in the vicinity of AChR-release sites. Second, OIG-4 might behave as a negative regulator of L-AChR activity. In this case, the partial declustering observed in *oig-4* mutants could be offset by augmentation of L-AChR activity in the absence of OIG-4. However, this hypothesis would also predict an increased response to pressure-applied levamisole, which activates the total number of receptors present in synaptic and extrasynaptic regions. Such an increase is not observed in *oig-4* null mutants. Third, pre-synaptic release might be enhanced in *oig-4*

mutants. To test this hypothesis, we measured quantal size and quantal content at cholinergic NMJs and found no difference between the wild-type and *oig-4* mutants, suggesting that pre-synaptic release was not enhanced (data not shown). A remaining hypothesis is a decrease in acetylcholinesterase (AChE) activity at NMJs of *oig-4* mutants. As in mammals, AChE concentrate at NMJs based on histochemical detection (Culotti *et al*, 1981). If the amount of AChE is decreased at the NMJs of *oig-4* mutants, this would cause an increased amount of ACh in the synaptic cleft which might, in turn, compensate for the decreased density of receptors near ACh-release sites. However, if ACh clearance would be decreased in *oig-4* mutants, the size or the kinetics of the N-AChR-dependent evoked response should be modified, which we did not observe (data not shown). Yet, this negative result does not formally rule out a partial decrease of AChE activity at the synapse. Unfortunately, no reagent is available to directly assess the protein distribution of the four AChEs encoded in the worm genome. Therefore, understanding the relationship between AChR and AChE clustering remains to be addressed at the *C. elegans* NMJ.

A multi-modular extracellular complex for AChR clustering

So far three proteins with distinct domains have been demonstrated to be required for L-AChR clustering. LEV-9 function relies on CCP domains, LEV-10 on CUB domains and OIG-4 likely on a single Ig domain. Interestingly, such domains are highly represented in proteins of the vertebrate immune system. However, they are also present in numerous genes expressed in neurons. For example, we noticed a high prevalence of genes encoding both CUB and CCP domains in mouse and human databases, about half of which are expressed in the brain (Marie Gendrel and JLB, unpublished data). Ig and CCP domains are also combined in some neuronal proteins. For example, the human gene *SPRX2*, mutation of which causes epilepsy and mental retardation, encodes a secreted protein containing three CCP and one Ig-related domains (Roll *et al*, 2006).

CUB, CCP and Ig domains can all mediate protein–protein interactions and indeed, our results indicate that OIG-4, LEV-9 and LEV-10 do form a physical complex containing L-AChRs. Specifically, OIG-4 co-immunoprecipitates L-AChRs and LEV-10, and a direct interaction between LEV-9 and LEV-10 has been demonstrated in a heterologous system (Gendrel *et al*, 2009). However, such a direct interaction between OIG-4 and LEV-10 could not be detected in the same system (data not shown). Analysis of these different proteins in mutant backgrounds unmasks non-equivalent functions. LEV-9, LEV-10 and L-AChRs are strictly codependent for their synaptic localization and can form small, infrequent clusters in the absence of OIG-4. This suggests that these three proteins form an obligatory core complex supporting the synaptic localization of L-AChRs. However, the stability of this complex is directly or indirectly regulated by OIG-4 since in *oig-4* mutants L-AChRs and LEV-10 are expressed, yet they can no longer be co-immunoprecipitated. Reciprocally, OIG-4 is no longer detected by immunofluorescence in the absence of L-AChRs, suggesting a direct interaction between these two proteins, yet OIG-4 remains detectable at low levels in synaptic regions of *lev-9* and *lev-10* mutants indicating that it binds cue(s) enriched at the synapse.

As LEV-9 and LEV-10 co-cluster with L-AChRs but inefficiently localize at the synapse on one hand, and OIG-4 localizes at the synapse but inefficiently recruits L-AChRs on the other hand, cooperative interactions between these components are likely to occur at the synapse to achieve proper localization of the receptors. Many scenarios can be envisioned at this stage. For example, an interaction between OIG-4 and LEV-9 or LEV-10 might convert a binding site for a synaptic cue from low to high affinity. Such an interaction between an Ig-like domain, a CCP domain and a carbohydrate moiety was demonstrated to stabilize the physical interaction between L1 and neurocan (Oleszewski *et al*, 2000). OIG-4 might also be required to directly stabilize the L-AChR/LEV-9/LEV-10 complex. In mammals, factor H, a regulator of complement activation, contains 20 CCP domains (Kristensen and Tack, 1986; Schmidt *et al*, 2008a). Intramolecular interactions of factor H, in the fluid phase, are thought to be disrupted by interactions of its C-terminus with the cell membrane, unmasking complement-regulatory sites contained in the N-terminal region of the protein (Schmidt *et al*, 2008b). By analogy, it is conceivable that OIG-4 binding to LEV-9 or LEV-10 causes conformational changes that unmask additional binding sites and stabilize the L-AChR/LEV-9/LEV-10 complex. Of course, none of the models described above are exclusive. Precise identification of the domains engaged in molecular interactions among each of the different partners and *in vitro* reconstitution of this macromolecular complex will eventually be required to refine a molecular scenario.

Materials and methods

Strains were maintained at 20°C on NG agar plates under standard conditions (Brenner, 1974). OP50 *E. coli* was generally used for feeding, except for strains prepared for biochemistry, which were maintained on enriched peptone plates with HB101 *E. coli*. Strains, molecular constructs and transgenes used are described in the Supplementary data.

Levamisole assay

Assays for levamisole sensitivity after acute and overnight exposure were performed as previously described (Gendrel *et al*, 2009). Further details are provided in the Supplementary data.

EMS mutagenesis—screens for levamisole resistance

EMS mutagenesis was as previously described (Brenner, 1974). Animals were screened for acute or overnight resistance to levamisole at the F2 generation. Mutants were out-crossed at least 6 times. For non-complementation screens, N2 wild-type males were mutagenized with EMS. After overnight recovery, they were crossed into *oig-4(kr39); rol-6(e187)* hermaphrodites. Parental individuals (P0s) were transferred to fresh plates every 12–24 h for 3 days in order to synchronize their progeny. Adult F1s were transferred to 0.6 mM levamisole plates. After overnight exposure, resistant animals derived from the cross-progeny were identified as non-roller survivors and transferred onto fresh plates. Approximately 24 000 haploid genomes were screened. A new mutation was identified after PCR amplification and sequencing of the *oig-4* genomic locus. *oig-4(kr193)* was out-crossed at least 6 times.

Electrophysiology

Electrophysiological methods were as previously described (Richmond and Jorgensen, 1999; Gendrel *et al*, 2009). N-AChR analysis was performed in an *unc-49(e407)* background to eliminate currents caused by the activation of GABA receptors. L-AChR-evoked recordings analysis was performed in an *unc-49(e407); acr-16(ok789)* background to eliminate currents arising from the activation of GABA receptors and N-AChRs.

Immunocytochemical staining

Worms were prepared by the freeze-crack method described previously (Duerr *et al*, 1999; Gendrel *et al*, 2009). Further details are provided in the Supplementary data.

Protein extraction

The LEV-10 protein was detected in low speed supernatants (LSS) of mixed staged populations after protein extraction. Worms (2 ml) were isolated using sucrose flotation (in 2 M sucrose solution) to remove bacteria and debris and then frozen in pellets at −80°C until use. The protein extraction and preparation of the LSS were performed as previously described (Gendrel *et al*, 2009).

For UNC-29 and tubulin detection, mixed staged populations were collected from OP50 seeded NGM plates. They were rinsed with H_2O and allowed to sediment on ice, for four repeats to wash out bacteria. The pellets were solubilized in Laemmli buffer with 2% β-ME, sonicated for 1 min and boiled at 95°C for 10 min.

Immunoprecipitation

T7 IP and GFP IP for UNC-63-YFP was performed as described previously (Gendrel *et al*, 2009).

GFP IP (for GFP-OIG-4). The LSS volume from 3 ml worm pellets was brought up to 15 ml with homogenization buffer supplemented with 100 mM NaCl and 1% Triton TX-100. Either 40 μl of GFP-Trap_A conjugated beads (chromotek) or 15 μl of mouse anti-GFP monoclonal antibodies (JL-8 Clontech, dilution 1:1000) with 20 μl of Protein G sepharose beads (Sigma) were mixed with the supernatant overnight at 4°C. The beads were then collected and washed subsequently once with buffer (50 mM Hepes pH 7.7, 50 mM KCl, 2 mM $MgCl_2$, 250 mM sucrose, 1 mM EDTA pH 8, 100 mM NaCl, 1% Triton TX-100) and once with buffer (50 mM Hepes pH 7.7, 50 mM NaCl). Laemmli buffer without β-ME was added to the beads; the supernatant was collected and 2% β-ME was then added. The eluted fraction was kept at −20°C and used for western blotting (for detection of GFP-OIG-4 IP or of UNC-29 and LEV-10 co-IP).

Western blotting

Western blotting membranes were probed with purified rabbit antibodies anti-LEV-10 (dilution 1:250) or anti-UNC-29 (dilution 1:500) or commercial mouse antibodies DH1a (Sigma, dilution 1:5000) or mouse anti-GFP monoclonal antibodies (JL-8 Clontech, dilution 1:2500), or mouse anti-T7 monoclonal antibodies (Novagen, dilution 1:10000) and secondary Horseradish-peroxidase-conjugated goat anti-rabbit or goat anti-mouse antibodies (DAKO, dilution 1:50) and revealed with LumiLight reagents (Roche).

Supplementary data

Supplementary data are available at *The EMBO Journal* Online (http://www.embojournal.org).

Acknowledgements

We thank the Caenorhabditis Genetic Center, the International *C. elegans* Gene Knock-out Consortium and the Japanese National BioResources Project for strains. We also thank A Fire, J Rand and L Pintard for reagents; B Matthieu and H Gendrot for technical help; V Promponas for help in bioinformatics; S Marty for critical reading of the manuscript. GR was supported by a fellowship from the Ministère de la Recherche and by the Association Francaise Contre les Myopathies. This work was funded by INSERM, the Agence Nationale de la Recherche (ANR-07-NEURO-032-01) and the Association Française contre les Myopathies. JR was supported by NIH RO1 MH073156.

Author contributions: GR performed most of the experiments except the electrophysiology experiments performed by JER and the initial screen performed by J-LB. GR and J-LB wrote the manuscript and J-LB supervised the project.

Conflict of interest

The authors declare that they have no conflict of interest.

References

Besse F, Mertel S, Kittel RJ, Wichmann C, Rasse TM, Sigrist SJ, Ephrussi A (2007) The Ig cell adhesion molecule Basigin controls compartmentalization and vesicle release at Drosophila melanogaster synapses. *J Cell Biol* **177:** 843–855

Biederer T, Sara Y, Mozhayeva M, Atasoy D, Liu X, Kavalali ET, Südhof TC (2002) SynCAM, a synaptic adhesion molecule that drives synapse assembly. *Science* **297:** 1525–1531

Bjartmar L, Huberman AD, Ullian EM, Rentería RC, Liu X, Xu W, Prezioso J, Susman MW, Stellwagen D, Stokes CC, Cho R, Worley P, Malenka RC, Ball S, Peachey NS, Copenhagen D, Chapman B, Nakamoto M, Barres BA, Perin MS (2006) Neuronal pentraxins mediate synaptic refinement in the developing visual system. *J Neurosci* **26:** 6269–6281

Boulin T, Gielen M, Richmond J, Williams D, Paoletti P, Bessereau J (2008) Eight genes are required for functional reconstitution of the Caenorhabditis elegans levamisole-sensitive acetylcholine receptor. *Proc Natl Acad Sci USA* **105:** 18590–18595

Brenner S (1974) The genetics of Caenorhabditis elegans. *Genetics* **77:** 71–94

Cho RW, Park JM, Wolff SBE, Xu D, Hopf C, Kim J-A, Reddy RC, Petralia RS, Perin MS, Linden DJ, Worley PF (2008) mGluR1/5-dependent long-term depression requires the regulated ectodomain cleavage of neuronal pentraxin NPR by TACE. *Neuron* **57:** 858–871

Cox EA, Tuskey C, Hardin J (2004) Cell adhesion receptors in C. elegans. *J Cell Sci* **117:** 1867–1870

Culotti JG, Von Ehrenstein G, Culotti MR, Russell RL (1981) A second class of acetylcholinesterase-deficient mutants of the nematode Caenorhabditis elegans. *Genetics* **97:** 281–305

Dalva MB, Takasu MA, Lin MZ, Shamah SM, Hu L, Gale NW, Greenberg ME (2000) EphB receptors interact with NMDA receptors and regulate excitatory synapse formation. *Cell* **103:** 945–956

Duerr JS, Frisby DL, Gaskin J, Duke A, Asermely K, Huddleston D, Eiden LE, Rand JB (1999) The cat-1 gene of Caenorhabditis elegans encodes a vesicular monoamine transporter required for specific monoamine-dependent behaviors. *J Neurosci* **19:** 72–84

Eimer S, Gottschalk A, Hengartner M, Horvitz HR, Richmond J, Schafer WR, Bessereau J-L (2007) Regulation of nicotinic receptor trafficking by the transmembrane Golgi protein UNC-50. *EMBO J* **26:** 4313–4323

Elias GM, Nicoll RA (2007) Synaptic trafficking of glutamate receptors by MAGUK scaffolding proteins. *Trends Cell Biol* **17:** 343–352

Fares H, Greenwald I (2001) Genetic analysis of endocytosis in Caenorhabditis elegans: coelomocyte uptake defective mutants. *Genetics* **159:** 133–145

Fleming JT, Squire MD, Barnes TM, Tornoe C, Matsuda K, Ahnn J, Fire A, Sulston JE, Barnard EA, Sattelle DB, Lewis JA (1997) Caenorhabditis elegans levamisole resistance genes lev-1, unc-29, and unc-38 encode functional nicotinic acetylcholine receptor subunits. *J Neurosci* **17:** 5843–5857

Francis MM, Evans SP, Jensen M, Madsen DM, Mancuso J, Norman KR, Maricq AV (2005) The Ror receptor tyrosine kinase CAM-1 is required for ACR-16-mediated synaptic transmission at the C. elegans neuromuscular junction. *Neuron* **46:** 581–594

Gally C, Eimer S, Richmond JE, Bessereau J-L (2004) A transmembrane protein required for acetylcholine receptor clustering in Caenorhabditis elegans. *Nature* **431:** 578–582

Gautam M, Noakes PG, Moscoso L, Rupp F, Scheller RH, Merlie JP, Sanes JR (1996) Defective neuromuscular synaptogenesis in agrin-deficient mutant mice. *Cell* **85:** 525–535

Gendrel M, Rapti G, Richmond JE, Bessereau J-L (2009) A secreted complement-control-related protein ensures acetylcholine receptor clustering. *Nature* **461:** 992–996

Gerrow K, El-Husseini A (2007) Receptors look outward: revealing signals that bring excitation to synapses. *Sci STKE* **2007:** pe56

Henderson JT, Georgiou J, Jia Z, Robertson J, Elowe S, Roder JC, Pawson T (2001) The receptor tyrosine kinase EphB2 regulates NMDA-dependent synaptic function. *Neuron* **32:** 1041–1056

Huh K-H, Fuhrer C (2002) Clustering of nicotinic acetylcholine receptors: from the neuromuscular junction to interneuronal synapses. *Mol Neurobiol* **25:** 79–112

Kneussel M, Loebrich S (2007) Trafficking and synaptic anchoring of ionotropic inhibitory neurotransmitter receptors. *Biol Cell* **99:** 297–309

Kraut R, Menon K, Zinn K (2001) A gain-of-function screen for genes controlling motor axon guidance and synaptogenesis in Drosophila. *Curr Biol* **11:** 417–430

Kristensen T, Tack BF (1986) Murine protein H is comprised of 20 repeating units, 61 amino acids in length. *Proc Natl Acad Sci USA* **83:** 3963–3967

Lewis JA, Wu CH, Berg H, Levine JH (1980) The genetics of levamisole resistance in the nematode Caenorhabditis elegans. *Genetics* **95:** 905–928

O'Brien RJ, Xu D, Petralia RS, Steward O, Huganir RL, Worley P (1999) Synaptic clustering of AMPA receptors by the extracellular immediate-early gene product Narp. *Neuron* **23:** 309–323

Oleszewski M, Gutwein P, von der Lieth W, Rauch U, Altevogt P (2000) Characterization of the L1-neurocan-binding site. Implications for L1-L1 homophilic binding. *J Biol Chem* **275:** 34478–34485

Rammensee HG, Falk K, Rötzschke O (1993) Peptides naturally presented by MHC class I molecules. *Annu Rev Immunol* **11:** 213–244

Richmond JE, Davis WS, Jorgensen EM (1999) UNC-13 is required for synaptic vesicle fusion in C. elegans. *Nat Neurosci* **2:** 959–964

Richmond JE, Jorgensen EM (1999) One GABA and two acetylcholine receptors function at the C. elegans neuromuscular junction. *Nat Neurosci* **2:** 791–797

Roll P, Rudolf G, Pereira S, Royer B, Scheffer IE, Massacrier A, Valenti M-P, Roeckel-Trevisiol N, Jamali S, Beclin C, Seegmuller C, Metz-Lutz M-N, Lemainque A, Delepine M, Caloustian C, de Saint Martin A, Bruneau N, Depétris D, Mattéi M-G, Flori E *et al* (2006) SRPX2 mutations in disorders of language cortex and cognition. *Hum Mol Genet* **15:** 1195–1207

Rougon G, Hobert O (2003) New insights into the diversity and function of neuronal immunoglobulin superfamily molecules. *Annu Rev Neurosci* **26:** 207–238

Sanes JR, Lichtman JW (2001) Induction, assembly, maturation and maintenance of a postsynaptic apparatus. *Nat Rev Neurosci* **2:** 791–805

Schlimgen AK, Helms JA, Vogel H, Perin MS (1995) Neuronal pentraxin, a secreted protein with homology to acute phase proteins of the immune system. *Neuron* **14:** 519–526

Schmidt CQ, Herbert AP, Hocking HG, Uhrín D, Barlow PN (2008a) Translational mini-review series on complement factor H: structural and functional correlations for factor H. *Clin Exp Immunol* **151:** 14–24

Schmidt CQ, Herbert AP, Kavanagh D, Gandy C, Fenton CJ, Blaum BS, Lyon M, Uhrín D, Barlow PN (2008b) A new map of glycosaminoglycan and C3b binding sites on factor H. *J Immunol* **181:** 2610–2619

Shapiro L, Love J, Colman DR (2007) Adhesion molecules in the nervous system: structural insights into function and diversity. *Annu Rev Neurosci* **30:** 451–474

Shen K, Bargmann CI (2003) The immunoglobulin superfamily protein SYG-1 determines the location of specific synapses in C. elegans. *Cell* **112:** 619–630

Shen K, Fetter RD, Bargmann CI (2004) Synaptic specificity is generated by the synaptic guidepost protein SYG-2 and its receptor, SYG-1 (Erratum). *Cell* **117:** 553

Sheth N, Roca X, Hastings ML, Roeder T, Krainer AR, Sachidanandam R (2006) Comprehensive splice-site analysis using comparative genomics. *Nucleic Acids Res* **34:** 3955–3967

Sia G-M, Béïque J-C, Rumbaugh G, Cho R, Worley PF, Huganir RL (2007) Interaction of the N-terminal domain of the AMPA receptor GluR4 subunit with the neuronal pentraxin NP1 mediates GluR4 synaptic recruitment. *Neuron* **55:** 87–102

Song Y, Balice-Gordon R (2008) New dogs in the dogma: Lrp4 and Tid1 in neuromuscular synapse formation. *Neuron* **60:** 526–528

Takasu MA, Dalva MB, Zigmond RE, Greenberg ME (2002) Modulation of NMDA receptor-dependent calcium influx and gene expression through EphB receptors. *Science* **295:** 491–495

Touroutine D, Fox RM, Von Stetina SE, Burdina A, Miller DM, Richmond JE (2005) acr-16 encodes an essential subunit of the levamisole-resistant nicotinic receptor at the Caenorhabditis elegans neuromuscular junction. *J Biol Chem* **280:** 27013–27021

Tsui CC, Copeland NG, Gilbert DJ, Jenkins NA, Barnes C, Worley PF (1996) Narp, a novel member of the pentraxin family, promotes neurite outgrowth and is dynamically regulated by neuronal activity. *J Neurosci* **16:** 2463–2478

Xu D, Hopf C, Reddy R, Cho RW, Guo L, Lanahan A, Petralia RS, Wenthold RJ, O'Brien RJ, Worley P (2003) Narp and NP1 form heterocomplexes that function in developmental and activity-dependent synaptic plasticity. *Neuron* **39:** 513–528

Yamagata M, Sanes JR (2008) Dscam and Sidekick proteins direct lamina-specific synaptic connections in vertebrate retina. *Nature* **451:** 465–469

Yamagata M, Sanes JR (2010) Synaptic localization and function of Sidekick recognition molecules require MAGI scaffolding proteins. *J Neurosci* **30:** 3579–3588

Yamagata M, Weiner JA, Sanes JR (2002) Sidekicks: synaptic adhesion molecules that promote lamina-specific connectivity in the retina. *Cell* **110:** 649–660

